

PARTICLE DYNAMICS AT STAGNATION POINT DURING LONGITUDINAL BUNCH COMPRESSION OF HIGH CURRENT BEAMS*

T. Kikuchi[†], S. Kawata, Utsunomiya Univ., Utsunomiya 321-8585, Japan
 K. Horioka, Tokyo Institute of Technology, Yokohama 226-8502, Japan

Abstract

Beam dynamics around a stagnation point during a longitudinal pulse compression is numerically investigated by using a three dimensional multi-particle code developed with a reduced electric field model. A deformation of the beam particle distribution in the longitudinal phase space is observed during the beam transport with the pulse compression. An rms transverse emittance growth is additionally increased along the beam transport due to the disruption in the longitudinal distribution of the beam particle.

INTRODUCTION

An intense heavy-ion beam (HIB) is one influential candidate as the energy driver, and the physics of space-charge-dominated beams is crucial in heavy ion inertial fusion (HIF) researches [1]. Required parameter values of HIB are several GeV particle energy, ~ 100 kA total current, and ~ 10 ns short pulse duration [2]. The beam parameters are far from those of conventional particle accelerator system. Therefore the beam dynamics and control are important research issues in HIF.

Not only for HIF application, but also research fields on high energy density physics (HEDP) and warm dense matter (WDM) sciences [3] driven by HIB illuminations require the generation of a high-current HIB [4].

At the final stage, the beam pulse must be longitudinally compressed from ~ 100 to ~ 10 ns. Induction voltage modulators, which have a precise waveform controllability, are useful devices for the bunch compression [5]. For an effective target implosion, we should transport and compress the bunch of HIB with a low emittance growth. For this reason, the final pulse compression and the final focusing are a key technology in the HIF driver system. In these regions, the intense HIB is in the space-charge-dominated state, and beam instabilities may occur during the beam transport.

In our previous studies [6, 7], the beam dynamics was investigated by using a two dimensional multi-particle code including the longitudinal pulse compression model. In this study, we carry out numerical simulations by using a three dimensional particle code developed. The longitudinal and transverse beam parameter changes are discussed from the numerical simulation results during the pulse compression. Disruption of the longitudinal particle distribution is shown in the beam transport, and implies that an emittance growth

larger than one near center of the beam bunch and two-dimensional sliced code result is caused due to the longitudinal particle motions.

SIMULATION MODEL AND BEAM PARAMETERS

The calculation code used, which is based on a particle-in-cell (PIC) method [8], takes into account of a self-electrostatic and an external applied magnetic fields, and can be described in a three dimensional Cartesian coordinate. The particle motions are calculated in the fully three dimensional space by neglecting a self-magnetic field.

The electric field created due to the space charge is calculated by using the Poisson equation,

$$\nabla^2 \phi = \frac{\partial^2 \phi}{\partial x^2} + \frac{\partial^2 \phi}{\partial y^2} + \frac{\partial^2 \phi}{\partial z^2} = -\frac{\rho}{\epsilon_0}, \quad (1)$$

where ϕ is the electrostatic potential, ρ is the charge density, and ϵ_0 is the permittivity of free space. By solving Eq. (1), the electric field can be completely determined by $\mathbf{E} = -\nabla\phi$, however the higher computational cost is unaffordable for a lot of parameter studies. Vorobiev and York proposed a sub-three-dimensional PIC method [9], and the approach is as follows. The three dimensional Poisson equation Eq. (1) can be replaced as

$$\frac{\partial^2 \phi}{\partial x^2} + \frac{\partial^2 \phi}{\partial y^2} = -\rho', \quad (2)$$

where

$$\rho' = \frac{\rho}{\epsilon_0} - \frac{\partial E_z}{\partial z}. \quad (3)$$

If Eq. (3) can be solved with including the transverse information, we can obtain the transverse electric field by solving the two dimensional Poisson equation as shown in Eq. (2).

Assuming the large aspect ratio to longitudinal and transverse directions for the beam bunch, we employ the simplified calculation model for the longitudinal electric field in this study. The transverse electric fields are normally calculated by $E_x = -\partial\phi/\partial x$ and $E_y = -\partial\phi/\partial y$, while by assuming the long wave approximation the longitudinal electric field can be given as

$$E_z = -\frac{g}{4\pi\epsilon_0\gamma_0^2} \frac{d\lambda}{dz}, \quad (4)$$

where γ_0 is the relativistic factor at the central energy for the beam and λ is the line charge density. For a space-charge dominated regime, g is the geometry factor defined

* Work supported by Japan Society for the Promotion of Science KAKENHI No.17740361.

[†] tkikuchi@cc.utsunomiya-u.ac.jp

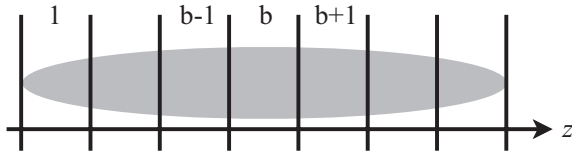


Figure 1: Sliced bunch model for the self-electric field calculations.

by

$$g \sim \log \frac{r_p^2}{r_x r_y}, \quad (5)$$

where r_p is the outer boundary pipe radius, r_x and r_y are effective beam radii estimated as

$$r_x = 2\sqrt{\langle (x_p - \langle x_p \rangle)^2 \rangle}, \quad (6)$$

with analogous expression for r_y . Here x_p is the transverse position of the beam particle at the index p .

To reduce the computational cost, the beam bunch is longitudinally sliced and separated to calculate the transverse and longitudinal electric fields as shown in Fig. 1. At each time-step the bunches sliced are identified by using the index b . The transverse electric fields are calculated at each slice. For this reason, the horizontal and vertical electric fields are rewritten as $E_{xb} = -\partial \phi_b / \partial x$ and $E_{yb} = -\partial \phi_b / \partial y$ at each slice. Here the subscripts b indicate the sliced bunch index. The electrostatic potential at each slice can be calculated by

$$\frac{\partial^2 \phi_b}{\partial x^2} + \frac{\partial^2 \phi_b}{\partial y^2} = -\rho'_b, \quad (7)$$

where

$$\rho'_b = \frac{\rho_b}{\epsilon_0} - \frac{dE_{zb}}{dz}. \quad (8)$$

Here

$$\frac{dE_{zb}}{dz} = -\frac{1}{4\pi\epsilon_0\gamma_0^2} \frac{d}{dz} \left(g_b \frac{d\lambda_b}{dz} \right). \quad (9)$$

The Poisson equation at each slice can be numerically solved by using a multigrid and SOR methods [10].

The beam parameters are assumed as Table 1 [2]. The

Table 1: Beam parameters.

Ion species	Pb ¹⁺
Number of ions	6.25×10^{14}
Particle energy [GeV]	10
Initial beam current [A]	400
Final beam current [kA]	10
Initial pulse duration [ns]	250
Final pulse duration [ns]	10

initial generalized perveance is assumed to be 3.58×10^{-6} . The initial undepressed and depressed phase advances are $\sigma_0 = 72$ deg and $\sigma = 65.2$ deg at 3 m in the longitudinal direction. A continuous focusing (CF) configuration is

assumed for the transverse confinement system. The transverse focusing coefficients $k_x = k_y = 0.157 \text{ m}^{-2}$ are constant for the CF model.

The transverse calculation region is fixed at the square of $10 \text{ cm} \times 10 \text{ cm}$, and the outer boundary condition is given as a conductor wall. As a result, the pipe radius r_p is assumed as 5 cm in this study.

The rms matched Gaussian [11] beam is chosen as the initial particle (non-stationary) distribution for the transverse plane. The longitudinal charge distribution is assumed to be uniform before the bunch compression, on which a head-to-tail velocity tilt $(\beta_t - \beta_h)/\beta_c$ of 5 % is applied. Here β_h , β_t , and β_c are the velocity divided by light speed at the head, in the tail part and in the center of the beam, respectively.

LONGITUDINAL AND TRANSVERSE BEAM PARAMETERS DURING PULSE COMPRESSION

We simulate numerically the beam dynamics during the pulse compression with the CF focusing model as discussed in the previous section.

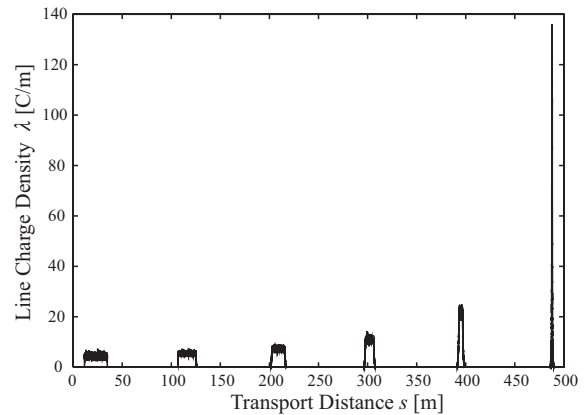


Figure 2: Line charge density along the beam transport direction.

Figure 2 shows the line charge density profiles at each longitudinal position during the beam transport. Due to the head-to-tail velocity tilt given initially, the beam bunch is longitudinally compressed during the transport, and the line charge density can be increased with the pulse compression.

The emittance value can be used to evaluate the beam quality. We define the average of unnormalized rms transverse emittance as $\varepsilon = (\varepsilon_{x,rms} + \varepsilon_{y,rms})/2$, where $\varepsilon_{x,rms}$ and $\varepsilon_{y,rms}$ are the unnormalized rms emittances for horizontal and vertical directions given by

$$\varepsilon_{x,rms} = [\langle x_p^2 \rangle \langle x_p'^2 \rangle - \langle x_p x_p' \rangle]^2, \quad (10)$$

and

$$\varepsilon_{y,rms} = [\langle y_p^2 \rangle \langle y_p'^2 \rangle - \langle y_p y_p' \rangle]^2, \quad (11)$$

where the prime (\prime) indicates the slope, i.e., $x'_p = dx_p/dz_p$ and $y'_p = dy_p/dz_p$, respectively. The initial emittance ε_i is assumed to be $\varepsilon_i = 10$ mm-mrad, and $\varepsilon_{x,rms} = \varepsilon_{y,rms} = \varepsilon_i$. The evolutions of the emittance growth $\varepsilon/\varepsilon_i$, which indicates the ratio of the average emittance to the initial one along the transport distance, are shown in Fig. 3. The emittance growth over the entire beam is calculated by considering all beam particles, and the emittance growth near center is evaluated by the particles included in the range of ± 10 cm fixed from the longitudinal center of the beam bunch. As shown in Fig. 3, the emittance growth evaluated near center of the beam bunch is lower than one over the entire beam bunch. We also calculate the particle dynamics in the transverse cross section of the beam bunch, and the effect of the longitudinal compression is performed as the current increase model. As shown in Fig. 2, the beam current is increased as $1/z_b(s)$, where z_b is the half bunch length at each transport distance s . For this reason, the beam current increase model is assumed to calculate the 2D sliced bunch. It is found that the 2D sliced calculation with the longitudinal compression model well represents the emittance growth history for the 3D calculation result.

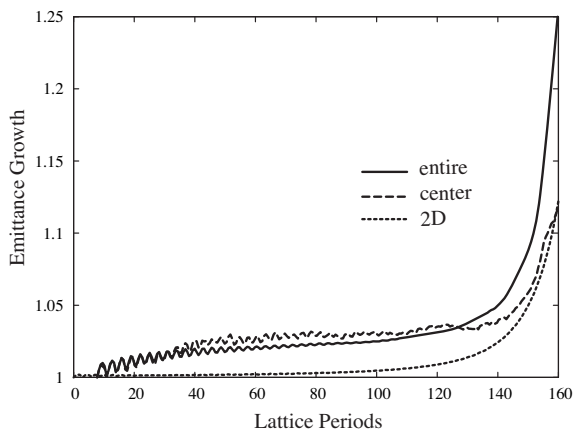


Figure 3: Evolution of the rms emittance during the beam transport with the pulse compression. The solid curve indicates the emittance growth over the entire beam bunch, the dashed line shows one evaluated near center of the beam bunch, and the dotted line shows for the 2D sliced calculation result with the longitudinal compression model.

Figure 4 shows the normalized charge distribution in the longitudinal phase space at the stagnation point. A disruption of the smooth particle distribution in the longitudinal phase space is indicated by Fig. 4. The disruption is caused by increasing the amplitude of the longitudinal electric field due to the pulse compression. As a result, the large transverse emittance growth over the entire beam bunch can be caused due to the disruption of the particle distribution in the longitudinal phase space as shown in Fig. 4.

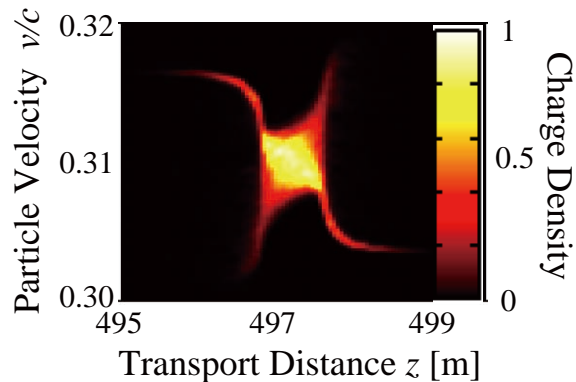


Figure 4: Normalized charge distribution in the longitudinal phase space at the stagnation point.

CONCLUSIONS

A high-current HIB dynamics during the beam transport with a longitudinal pulse compression was numerically investigated by using a three dimensional particle simulation code. The used code was developed to solve the three dimensional particle motions with the reduced electric field due to the space charge effect and the applied external magnetic field for the transverse confinement of the beam.

A disruption of smooth particle distribution in a longitudinal phase space during the pulse compression, which is caused due to the longitudinal self-electric field, was observed. A comparison of emittance growth between the all particles in the beam bunch, the particles included near center of the beam bunch and 2D sliced calculation result implies that the rms emittance growth over the entire beam can be increased due to the disruption of the longitudinal particle distribution.

REFERENCES

- [1] J.J. Barnard, *J. Fusion Energy* **17**, 223 (1998).
- [2] J.J. Barnard, et al., *Nucl. Instrum. Methods in Phys. Res.* **A415**, 218 (1998).
- [3] T. Sasaki, Y. Yano, M. Nakajima, T. Kawamura, K. Horioka, *Nucl. Instrum. Methods in Phys. Res.* **A 577**, 313 (2007).
- [4] K. Horioka, et al., *Nucl. Instrum. Methods in Phys. Res.* **A 577**, 298 (2007).
- [5] K. Horioka, et al., *Laser Part. Beams* **20**, 609 (2002).
- [6] T. Kikuchi, M. Nakajima, K. Horioka, and T. Katayama, *Phys. Rev. ST Accel. Beams* **7**, 034201 (2004).
- [7] T. Kikuchi, K. Horioka, M. Nakajima, S. Kawata, *Nucl. Instrum. Methods in Phys. Res.* **A 577**, 103 (2007).
- [8] R.W. Hockney and J.W. Eastwood, *Computer Simulation Using Particles*, McGraw-Hill, New York, (1981).
- [9] L.G. Vorobiev and R.C. York, *Phys. Rev. ST Accel. Beams* **3**, 114201 (2000).
- [10] U. Trottenberg, C.W. Oosterlee, and A. Schüller, *MULTI-GRID*, Elsevier, San Diego, (2001).
- [11] Y.K. Batygin, *Nucl. Instrum. Methods in Phys. Res.* **A 539**, 455 (2005).